Title
Small Heat Shock Protein Suppression of Vpr-Induced Cytoskeletal Defects in Budding Yeast

Journal
Molecular and Cellular Biology, 17(7)

ISSN
0270-7306

Authors
Gu, Jirong
Emerman, Michael
Sandmeyer, Suzanne

Publication Date
1997-07-01

DOI
10.1128/mcb.17.7.4033

MOLECULAR AND CELLULAR BIOLOGY, July 1997, p. 4033–4042 Vol. 17, No. 7
0270-7306/97/$04.00+0

Small Heat Shock Protein Suppression of Vpr-Induced Cytoskeletal Defects in Budding Yeast

JIRONG GU,[1]† MICHAEL EMERMAN,[2] AND SUZANNE SANDMEYER[1]*

Department of Microbiology and Molecular Genetics, College of Medicine, University of California, Irvine, California 92697-4025,[1] and Division of Molecular Medicine, Fred Hutchinson Cancer Research Center, Seattle, Washington 98104[2]

Received 19 November 1996/Returned for modification 23 December 1996/Accepted 6 April 1997

Expression of the auxiliary human immunodeficiency virus type 1 (HIV-1) protein Vpr causes arrest of primate host cells in G_2. Expression of this protein in budding yeast has been previously reported to cause growth arrest and a large-cell phenotype. Investigation of the effect of Vpr expression in budding yeast, reported here, showed that it causes disruption of the actin cytoskeleton. Expression of *HSP42*, the gene for a small heat shock protein (sHSP), from a high-copy-number plasmid reversed this effect. The sHSPs are induced by exposure of cells to thermal, osmotic, and oxidative stresses and to mitogens. In animal cells, overexpression of sHSPs causes increased resistance to stress and stabilization of actin stress fibers. Yeast cells subjected to mild stress, such as shifting from 23 to 39°C, arrest growth and then resume cell division. Growth arrest is accompanied by transient disorganization of the cytoskeleton. Yeast in which the *HSP42* gene was disrupted and which was subjected to moderate thermal stress reorganized the actin cytoskeleton more slowly than did wild-type control cells. These results demonstrate that in yeast, as in metazoan cells, sHSPs promote maintenance of the actin cytoskeleton.

Vpr is a 14-kDa protein encoded by human immunodeficiency virus type 1 (HIV-1) that mediates at least two unusual properties of the virus. First, Vpr participates with the matrix protein in targeting the HIV preintegration complex into the nucleus of infected cells (22, 25). Second, Vpr causes infected cells to accumulate in G_2 of the cell cycle by blocking the activation of the mitotic cyclin-dependent kinase (6, 24, 28, 44). However, recent studies with the related simian immunodeficiency virus suggest that the two functions of Vpr are separable (21). The mechanisms through which Vpr exerts its effects are not well understood, and although cellular proteins which bind to Vpr have been identified (9, 45, 54), none fully explain its activities (18). The current study was undertaken in order to examine Vpr function in the genetically tractable, single-celled eukaryote *Saccharomyces cerevisiae.*

Although *S. cerevisiae* is evolutionarily distant from the natural primate host of HIV, these organisms have fundamental features of cellular regulation in common. The similarity of many yeast proteins to their mammalian counterparts has made it possible to screen in yeast for proteins which block the toxicity of inappropriately expressed proteins. For example, this type of screen was used to identify proteins which interact with mammalian Ras (16). Because even sequestration of a negatively acting protein can produce positive results, a screen for genes which block cytotoxicity can be less demanding than a functional screen. Macreadie et al. (35, 36) showed that expression of HIV-1 Vpr in budding yeast increases the doubling time and causes cell enlargement and microcolony formation. Cells which overexpress Vpr are sensitive to high-osmotic-strength medium.

In yeast, in addition to Vpr expression, defects in the actin cytoskeleton can cause unusual morphology and osmotic sensitivity. In normal yeast cells, actin is essential for polar cell growth and secretion (13). Filamentous actin (F actin) occurs as cortical patches and actin cables. In unbudded cells, actin cortical patches form a ring surrounding the site of bud emergence. Later, cortical actin concentrates in the growing bud. Actin cables are found principally in the mother cell, extending along the axis of growth toward the emerging daughter cell. As the bud enlarges and bud growth becomes isotropic, rather than apical, the patches delocalize throughout the cortex of the mother and daughter cells. As cell division proceeds, actin concentrates in the neck between the separating cells.

In our study, a high-copy-number yeast library was screened in order to identify proteins which can block the toxicity of Vpr. Positive clones were anticipated to encode proteins which interact directly with Vpr or which act indirectly to reverse the effect of its expression in yeast. The characterization of one of these clones, which contains the gene for a small heat shock protein (sHSP), is described in this report.

Heat shock proteins (HSPs) are expressed constitutively or in response to various environmental stimuli (17). Although not highly conserved as a family, sHSPs have a common carboxyl-terminal motif, $GXLX_4P$, which is also found in the eye lens proteins α-crystallin and β-crystallin (reviewed in references 4 and 14). In addition to heat, osmotic, oxidative, and nutritional stresses, developmental signals can induce the expression of sHSPs. Artificially increasing expression of the mammalian sHSP genes by transfection confers resistance to temperature, osmotic, and oxidative stresses and stabilizes actin stress fibers. In vitro, sHSPs have been shown to act as chaperones (27) and to inhibit actin polymerization (39, 40, 43).

In *S. cerevisiae*, there are two sHSPs: Hsp26p (30) and Hsp42p (56). In addition, a 12-kDa protein, Hsp12p (41), is also produced under stress conditions and therefore is sometimes referred to as an sHSP. However, because it does not contain the α-crystallin motif, whether it has functions related to those of the sHSPs which have this motif is not clear.

* Corresponding author. Present address: Department of Biological Chemistry, College of Medicine, University of California, Irvine, CA 92697-1700. Phone: (714) 824-7571. Fax: (714) 824-2688. E-mail: SBSANDME@UCI.EDU.

† Present address: Department of Biological Chemistry, College of Medicine, University of California, Irvine, CA 92697-1700.

Surprisingly, disruption of *HSP12* and *HSP26*, or of *HSP26* and *HSP42*, causes no major defect in thermotolerance (41, 51, 56).

The absence of a phenotype has complicated the use of yeast in studies of sHSP function. Recovery of an sHSP gene in the current study not only offered potential insights into the mode of action of viral protein Vpr but also provided a dramatic synthetic phenotype resulting from expression of an sHSP in yeast. Moreover, Hsp42p was shown to stabilize the actin cytoskeleton both in cells expressing Vpr and in cells undergoing mild hyperthermic stress.

MATERIALS AND METHODS

Strains and culture conditions. The *S. cerevisiae* strains used in this study are YPH500 (*MAT*α *ura3-52 lys2-801 ade2-101 trp1-63 his3-*Δ*200 leu2-*Δ*1*) and YPH501, which is a MATα/**a** diploid but otherwise isogenic with YPH500. These strains were constructed in the Hieter laboratory (48) and provided by M. Nomura (University of California, Irvine). Yeast transformations were performed by the lithium acetate procedure (26). Rich medium for *S. cerevisiae* cultures was YPD (1% yeast extract–2% peptone–2% dextrose) (23). When selection was necessary, synthetic dextrose (SD) medium (0.67% yeast nitrogen base–2% dextrose), synthetic galactose (SG) medium (0.67% yeast nitrogen base–2% galactose), or raffinose medium (0.67% yeast nitrogen base–2% raffinose) containing amino acids minus selective amino acids was used. Temperature shifts were performed with liquid cultures maintained in shaking water baths at the appropriate temperature.

Plasmids and recombinant constructs. Recombinant DNA techniques were performed essentially as described elsewhere (5). *vpr* from the LAI strain of HIV-1 and mutant *vpr* (F34I) were amplified by PCR and cloned into Bluescript (Stratagene) (46). The wild-type (wt) *vpr* clone was designated pPG-2. The *Pst*I-*Bam*HI fragments containing wt and mutant *vpr* were cloned into the yeast expression vector pYES2 (Invitrogen Corp.), resulting in plasmids pJG1495 and pJG1496, respectively. The pYES2 vector is a 2μm, high-copy-number plasmid marked with the yeast *URA3* gene and *Escherichia coli* Amp and ori. The expression of *vpr* on this plasmid was under the control of the galactose-inducible *GAL1-10* promoter. The yeast genomic library was cloned in the vector YEp351, a *LEU2*-marked high-copy-number plasmid, and was provided by J. Hirsch (Mt. Sinai Medical Center, New York, N.Y.) (19). Vpr suppressor plasmid pJG1508 (p*SUP1*) is a clone from the genomic library that contains a 7.1-kb *Sau*3A fragment from chromosome IV which encompasses three genes: Ty1 (*TYA*, *TYB*), *HSP42*, and *GST1*. Subclones were constructed in order to map the Vpr-suppressing activity. Plasmid pJG1497 contains a partial deletion of *GST1*. It was made by subcloning the 5.1-kb *Hin*dIII fragment of plasmid pJG1508 into YEp351. Plasmid pJG1498 contains a partial deletion of Ty1 and a partial deletion of *GST1*. It was made by subcloning the 3.6-kb *Pst*I fragment of plasmid pJG1508 into YEp351. Plasmid pJG1499 contains a partial deletion of Ty1 and a partial deletion of *HSP42*. It was made by excising a 2.9-kb *Nde*I fragment from plasmid pJG1508. Plasmid pJG1500 contains a deletion of *HSP42* and a partial deletion of *GST1*. It was produced by excising a 2.9-kb *Stu*I fragment from plasmid pJG1508. Plasmid pJG1501 has a +1 frameshift in the *HSP42* open reading frame (ORF); it was a derivative of pJG1498. The pJG1498 plasmid was digested with *Nde*I. The 5′ overhang was filled in with a polymerization reaction mediated by the DNA polymerase I large fragment (New England Biolabs). The resulting blunt-ended plasmid fragment was circularized by ligation with T4 ligase.

In order to obtain recombinant Hsp42p in amounts sufficient to use as an immunogen, the coding region was subcloned in frame into the bacterial expression vector pET15b (Novagen Inc.). The pET15b plasmid is a bacterial expression vector which encodes 6 consecutive histidine residues (His tag) that can be expressed at the N terminus of the target protein. An oligonucleotide with the sequence 5′-AGATCATACCAAGCCGAAGCCCGGGAATGAGTTTTTATC AACCATCC-3′ (coding strand) was used to add a *Sma*I restriction site (underlined in sequence) before the start codon of the *HSP42* ORF, resulting in plasmid pJG1400. Plasmid pJG1402 was made by cloning a 1.8-kb *Sma*I fragment of pJG1400 into pET15b cut by *Xho*I and made blunt in a reaction with the DNA polymerase I large fragment.

HSP26 was amplified in a PCR from yeast genomic DNA by using one primer (404), with the sequence 5′-CGGAATTCCGACTTAGCGCGTGCT-3′, and the other primer (405), with the sequence 5′-CGCGGATCCGCGTAGTCTGCTT TAATGTTG-3′, essentially as described previously (38). Approximately 7 ng of genomic DNA was used. The reaction was initiated by incubation at 95°C for 2 min and was continued with denaturation for 1 min at 94°C, annealing for 1.5 min at 65°C, and extension for 2 min at 72°C, for a total of 20 cycles. The reaction was completed by incubation for 5 min at 72°C. The PCR products were separated by electrophoresis on an agarose gel, and a fragment of the appropriate size was identified. This fragment was excised, isolated by batch purification with Geneclean (Bio 101 Inc.), and cloned into pCRII vector (Invitrogen Corp.). The identity of *HSP26* was confirmed by restriction digestion. *HSP26* was excised on an *Xba*I fragment and recloned into the *Xba*I site of the high-copy-number vector YEp351. This plasmid was designated pJG1504.

The *URA3* gene disruption system developed by Alani et al. (1) was used to disrupt the *HSP42* gene. The plasmid used consisted of a 3.8-kb fragment containing a functional yeast *URA3* gene flanked by *hisG* repeats from *Salmonella* sp. The *Sna*BI fragment from *HSP42* in pJG1498 was replaced with this 3.8-kb segment. The sequence containing *URA3* and flanking *hisG* repeats was excised on a fragment and exchanged for the corresponding region of wt *HSP42* in YPH501 by integrative transformation. These cells contained a single copy of *HSP42*, with *URA3* and flanking *hisG* repeats replacing internal *HSP42* sequence. Genomic DNA samples from this strain and the wt progenitor were digested with *Pvu*II and *Bgl*I, fractionated by electrophoresis, and probed with a radiolabeled *Eco*RI-*Pst*I fragment specific for *HSP42*. The wt allele yielded three fragments of 2.3, 3.1, and 0.8 kb, and the disrupted allele yielded a single 9.0-kb fragment. The resulting diploid Δ*hsp42* strain was sporulated. A haploid Δ*hsp42* isolate was identified by Southern analysis and designated YJG1136.

RNA analysis. Total RNA was glyoxylated (37) and separated by electrophoresis in a 1.1% agarose gel. The nucleic acid was transferred in a PosiBlot pressure blotter (Stratagene) essentially as described for Northern (RNA) blotting (52) to a Duralon-UV membrane and cross-linked in a UV Stratalinker 1800 (Stratagene). An *Xho*I-*Sna*BI fragment from the internal region of *HSP42* and a *Pst*I-*Bam*HI fragment from HIV-1 *vpr* in pPG-2 were labeled with [α-^{32}P]dATP by the random primer method (20). Filter-bound nucleic acid was hybridized to the probe, and the filter was washed as described previously (15) and exposed to Hyperfilm-MP (Amersham).

Whole-cell extraction. Yeast cells from 25-ml cultures, typically at an A_{600} of 0.8, were pelleted and washed in 3 ml of whole-cell extract (WCE) buffer consisting of 25 mM HEPES (pH 7.5), 5 mM $MgCl_2$, 0.1 mM EDTA, 50 mM KCl, and 10% glycerol. A mix of 250 μl of WCE buffer was brought to a concentration of 0.25 mM dithiothreitol (DTT) and supplemented with 4.2 μg of aprotinin for each sample. Cells were suspended in 180 μl of WCE buffer plus DTT and aprotinin and were vortexed with glass beads. Microcentrifuge tubes containing cells were vortexed at maximum speed for 15 s and then plunged into ice for 15 s. This procedure was repeated five times. After the liquid was transferred to a new tube, 70 μl of WCE buffer plus DTT and aprotinin was added to the tube containing the glass beads. The tube was vortexed again, and supernatant was pooled with the first extraction liquid and centrifuged in an Eppendorf microcentrifuge. The supernatant was transferred to a new tube. The protein concentration of the final extract was determined by Bradford assay (10).

Antisera. Polyclonal antisera against recombinant yeast Hsp42p were produced in a New Zealand White rabbit. *HSP42* was cloned into pET15b (pJG1402) as described above and expressed in BL21 cells (Novagen). An overnight culture was diluted 1:10 and grown at 37°C for 2 h. Hsp42p production was induced by the addition of isopropyl-1-thio-β-D-galactopyranoside (IPTG) to a concentration of 2 mM. After 5 h, cells were collected by centrifugation, lysed by sonication in 1 ml of lysis buffer (50 mM NaCl, 10 mM Tris [pH 8.0], 1 mM EDTA, and 6 M urea), and chilled on ice for 1 h. The lysate was centrifuged, and the supernatant was loaded onto a 1-ml nickel column (Pharmacia). After nonspecifically associated proteins were eluted in washing buffer (60 mM imidazole, 0.5 M NaCl, 20 mM Tris-HCl [pH 7.9], and 6 M urea), proteins were removed from the column in elution buffer (1 M imidazole, 0.5 M NaCl, 20 mM Tris-HCl [pH 7.9], 6 M urea). The eluted protein was fractionated by sodium dodecyl sulfate-polyacrylamide gel electrophoresis (SDS-PAGE). The region of the gel containing protein migrating in the approximate position of 42 kDa was excised and sent to Berkeley Antibody Company for rabbit immunization. Initially, 0.5 mg of Hsp42p in Freund's complete adjuvant was injected into the paralymph node region, with subsequent intramuscular booster injections of 0.25 mg in Freund's incomplete adjuvant every 3 weeks. Rabbits were bled 10 days after boosts. The immunoglobulin G (IgG) fraction was prepared from serum by chromatography over Sepharose-linked protein A.

Polyclonal anti-Vpr antisera were raised in a New Zealand White rabbit by using a recombinant maltose-binding protein–Vpr fusion protein produced in *E. coli* as the immunogen (29).

Immunoblot analysis. Proteins from WCE were fractionated by SDS-PAGE and transferred electrophoretically to Hybond-ECL membranes (Amersham) (53). The ECL system (Amersham) was used according to the manufacturer's instructions to detect proteins bound by the anti-Vpr or anti-Hsp42p antibodies.

Fluorescence microscopy. Fluorescence microscopy was carried out essentially as described elsewhere (42). For samples stained for F actin, cells were fixed in 3.7% formaldehyde and treated with a 1:2,000 dilution of tetramethyl rhodamine isothiocyanate (TRITC)-conjugated phalloidin (400 mg/ml; Sigma) (42). For samples in which Hsp42p and actin were both visualized, cells were fixed in 3.7% formaldehyde, the cell wall was digested with Zymolyase (Seikagaku Corp.) and Glusulase (Sigma), and cells were applied to polylysine-prepared slides and permeabilized with successive treatments of methanol and acetone. Hsp42p was reacted with the IgG fraction of rabbit anti-Hsp42p antisera at a dilution of 1:500, and actin was reacted with mouse anti-actin monoclonal antibody (International Chemicals and Nuclear Pharmaceuticals Inc.) at a dilution of 1:1,000. Rabbit IgG was detected with goat anti-rabbit IgG conjugated to fluorescein isothiocyanate (FITC) (Sigma) at a dilution of 1:1,000. Mouse IgG was detected with TRITC-conjugated goat anti-mouse IgG (Sigma) used at a 1:2,000 dilution. The mounting medium (90% glycerol and 1 mg of *p*-phenylenediamine [Sigma]/ml) included 1 mg of 4′,6-diamidino-2-phenylindole (DAPI; Sigma)/ml to allow visualization of DNA.

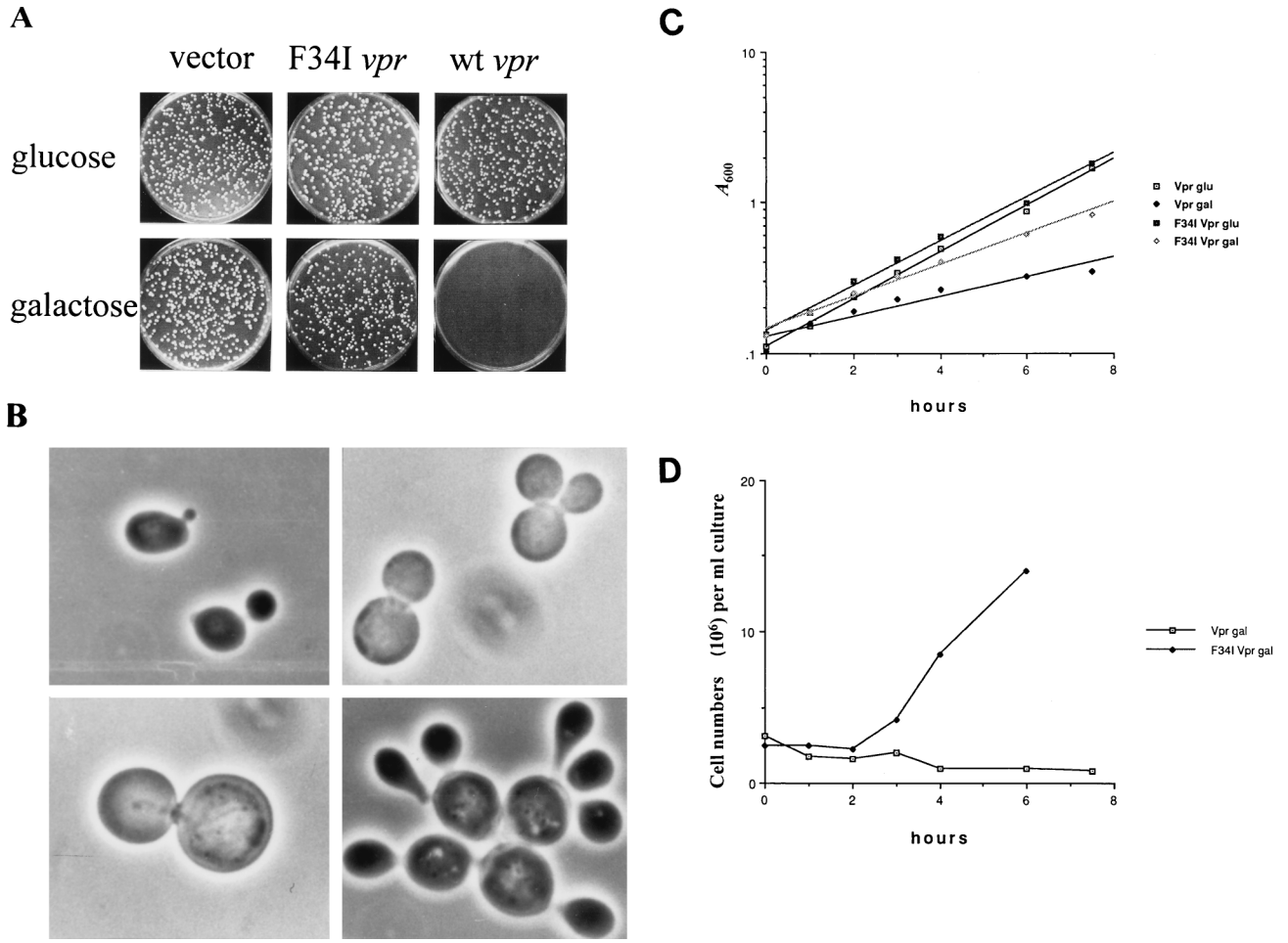

FIG. 1. Effects of expression of F34I *vpr* and wt *vpr* in yeast. (A) F34I *vpr* and wt *vpr* were cloned into a yeast expression vector, pYES2, in which *vpr* is under the control of the *GAL1-10* promoter. YPH500 cells with vector, F34I *vpr*, or wt *vpr* plasmids were plated on SD (uninduced *vpr*) or SG (induced *vpr*) medium and incubated at 30°C for 3 days (for SD medium) or 5 days (for SG medium). (B) YPH500 cells transformed with the galactose-inducible *vpr* plasmid were grown in SG (inducing) liquid medium for 0 (upper left), 6 (upper right), 24 (lower left), and 48 (lower right) h and were observed by phase-contrast microscopy. (C) YPH500 cells transformed with wt *vpr* or F34I *vpr* plasmid were grown to early exponential phase at 30°C in synthetic medium containing raffinose as a carbon source and lacking uracil. Glucose or galactose was added to the culture to repress or induce *vpr* expression. The A_{600} was measured at various time points. (D) Cells described in the legend to panel C were also plated on SD medium at 30°C for 3 days.

Fluorescence imaging was performed on a Nikon epifluorescence microscope with a Nikon 100× 1.25-numerical aperture plan objective. B-2A and G-1A filter cubes were used for observation of FITC and TRITC fluorochromes, respectively. Cells were photographed with TRI-X PAN 400 film (Kodak Co.).

RESULTS

Effects of Vpr expression in budding yeast. The effect of Vpr expression in budding yeast was investigated by expressing high levels of Vpr under the control of the *GAL1* promoter carried on the high-copy-number plasmid pJG1495. A *vpr* mutant in which the codon for phenylalanine at position 34 was changed to a codon for isoleucine (F34I), expressed from plasmid pJG1496, was also tested for ability to affect growth. The F34I mutant, like wt Vpr, arrests human cells in G_2. However, unlike wt Vpr, it is unable to target heterologous proteins to the nucleus (47a). In this vector context, *vpr* expression is repressed by glucose and induced by galactose. Strain YPH500 transformed with the plasmid carrying wt or mutant *vpr* genes or with vector alone was plated on SD or SG medium lacking uracil to select for the presence of the plasmid and was incubated at 30°C for 3 (SD) or 5 (SG) days. Expression of wt Vpr inhibited cell growth and resulted in microcolony formation (Fig. 1A). In contrast, expression of F34I Vpr had little effect.

Cells in which wt Vpr was expressed also showed an abnormal morphology (Fig. 1B). After more than 6 h, balloon-like cells with multiple buds accumulated in the culture. However, overexpression of F34I Vpr did not cause abnormal cell morphology (data not shown). The cell morphology observed in our strain upon expression of Vpr under the control of the *GAL1* promoter is similar to that reported by Macreadie et al. (36) for Vpr expression in their strain under regulation of the *CUP1* promoter. Budding yeast cells arrested in G_2 typically have a dumbbell shape resulting from retention of an enlarged bud. The phenotype observed in budding yeast cells expressing Vpr, therefore, was not due to a simple G_2 arrest. Fluorescence-activated cell sorting showed some accumulation of yeast cells in G_1 after 24 h of Vpr expression (data not shown).

In order to determine whether the effect of Vpr was cytostatic or cytocidal, the growth of cells expressing wt or F34I Vpr was monitored in liquid culture. Cells transformed with wt or F34I Vpr-expressing plasmids were grown in raffinose-containing synthetic medium lacking uracil to log phase, and either

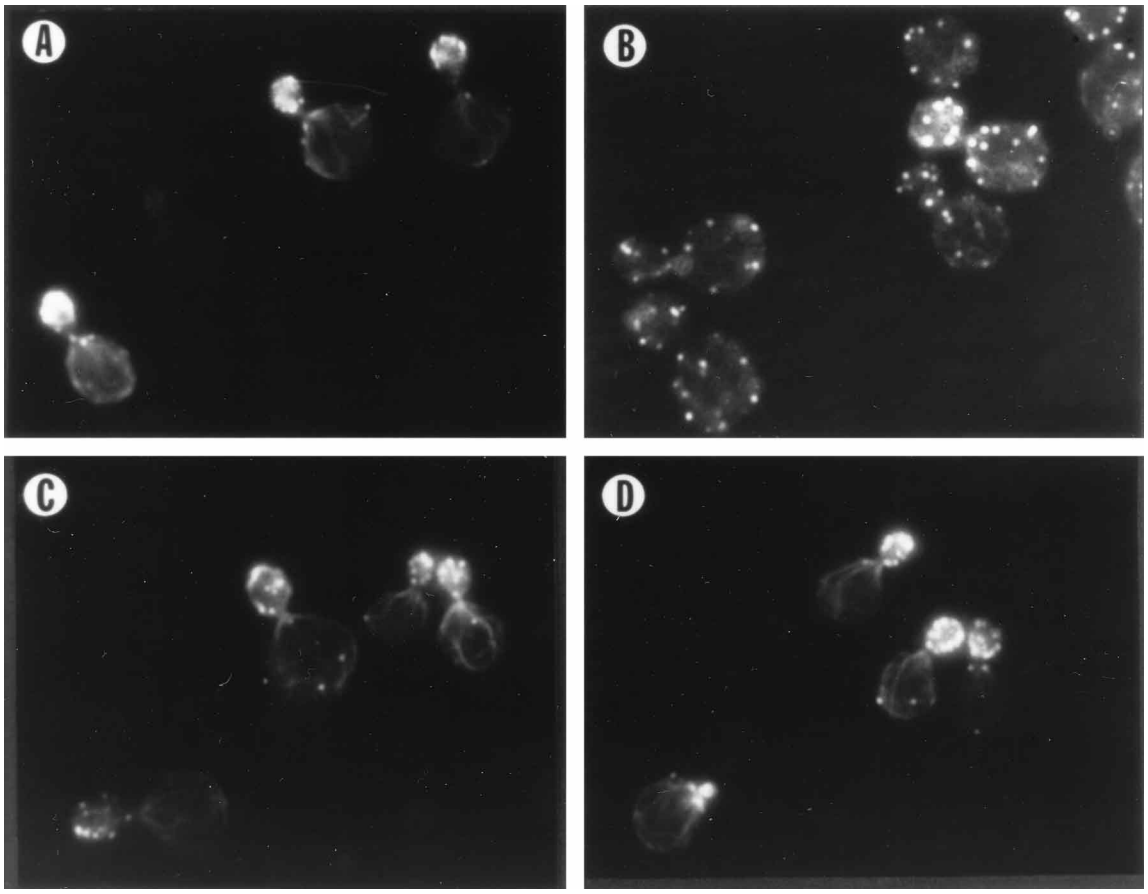

FIG. 2. Effect of Vpr expression on the actin cytoskeleton. YPH500 cells transformed with vector plasmids alone (A), wt *vpr* and vector plasmids (B), F43I *vpr* and vector plasmids (C), or wt *vpr* plasmid and *HSP42* plasmids (D) were grown in raffinose medium to log phase. Galactose was added to cultures for 7 h to induce Vpr expression. Cells were fixed, and F actin was stained with TRITC-phalloidin.

glucose (which repressed expression) or galactose (which induced expression) was added to the culture. The time required for the population to double in mass for cells expressing wt Vpr, determined by measuring A_{600}, was 2.5 times longer than that for cells expressing F34I Vpr (Fig. 1C). In order to determine the change in the number of viable cells in the culture, cells expressing Vpr were diluted from liquid culture onto SD lacking uracil, to repress expression, but to select for cells retaining the plasmid, and the number of colonies was determined. The total number of cells in the Vpr-expressing culture which retained the *URA3*-marked plasmid was approximately constant during the 7.5 h over which viability was monitored, indicating that Vpr was cytostatic rather than cytocidal (Fig. 1D). The modest increase in A_{600} of Vpr-expressing cells over this time course was consistent with the increased mass of individual cells observed by phase-contrast microscopy.

The observation that Vpr expression causes an enlarged cell morphology suggested that the cytoskeleton might be disrupted in Vpr-expressing yeast cells. Therefore, the effects of Vpr expression on the actin cytoskeleton structure were examined directly. Cells transformed with wt *vpr* or F34I *vpr* were grown in raffinose to log phase at 30°C. Glucose or galactose was added to cultures for 7 h to repress or induce *vpr* expression, respectively. Cells were fixed with 3.7% formaldehyde and stained with TRITC-phalloidin to visualize F actin. In control cells transformed with vector plasmids alone or plasmid carrying the F34I Vpr gene, mother cell actin cables were oriented toward the nascent bud and cortical patches of actin filaments in small-budded cells localized almost exclusively to the bud (Fig. 2A and C). In cells expressing wt Vpr, however, the actin cables were randomly oriented and the cortical actin filament patches were delocalized from the daughter cell to the mother cell (Fig. 2B).

Overexpression of sHSP suppresses Vpr toxicity in budding yeast. A high-copy-number yeast library in the *LEU2*-marked vector YEp351 was screened to identify genes for proteins which suppressed the cytostatic effect of Vpr. The library was transformed into cells containing the Vpr expression plasmid pJG1495 and plated on SG lacking uracil and leucine to select for cells that retained *vpr* and library clones, respectively. After retesting, seven suppressors were isolated out of an estimated 2×10^5 transformants. The growth of colonies containing wt Vpr in the presence of library vector alone and in the presence of one of the suppressors, p*SUP1*, is shown in Fig. 3A. The genomic library plasmid was rescued, and the sequence of the upstream end of the genomic insertion was determined. This sequence was used to perform a BLAST search (2) against GenBank.

The sequence of the p*SUP1* genomic insertion showed that it contained part of a Ty1 element, *HSP42*, and *GST1* (Fig. 3B). Four deletion subclones (pJG1497 to pIG1500) were constructed in order to map the region responsible for the suppressor activity. Plasmids pJG1497, which was lacking most of the *GST1* sequence, and pJG1498, which was lacking almost all of the Ty1 sequence, were both active as suppressors. Two other plasmids, pJG1499 and pJG1500, in which the Ty1-

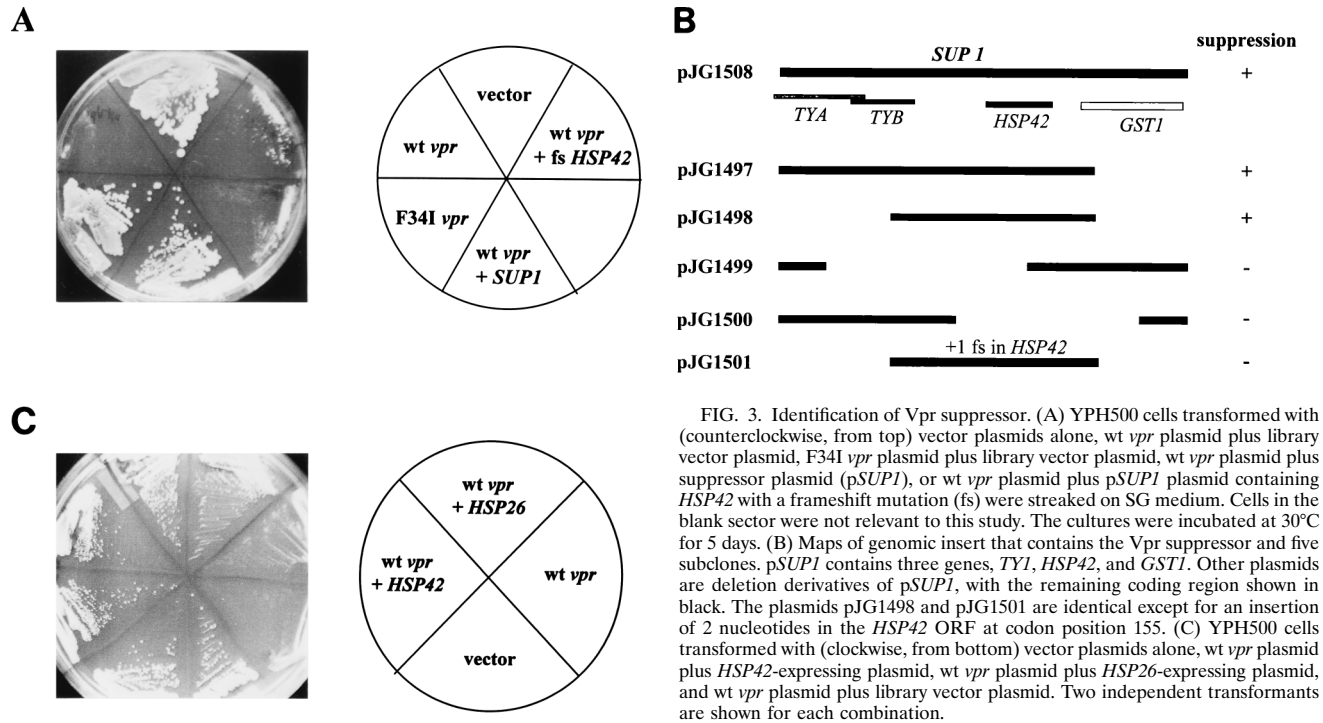

FIG. 3. Identification of Vpr suppressor. (A) YPH500 cells transformed with (counterclockwise, from top) vector plasmids alone, wt *vpr* plasmid plus library vector plasmid, F34I *vpr* plasmid plus library vector plasmid, wt *vpr* plasmid plus suppressor plasmid (p*SUP1*), or wt *vpr* plasmid plus p*SUP1* plasmid containing *HSP42* with a frameshift mutation (fs) were streaked on SG medium. Cells in the blank sector were not relevant to this study. The cultures were incubated at 30°C for 5 days. (B) Maps of genomic insert that contains the Vpr suppressor and five subclones. p*SUP1* contains three genes, *TY1*, *HSP42*, and *GST1*. Other plasmids are deletion derivatives of p*SUP1*, with the remaining coding region shown in black. The plasmids pJG1498 and pJG1501 are identical except for an insertion of 2 nucleotides in the *HSP42* ORF at codon position 155. (C) YPH500 cells transformed with (clockwise, from bottom) vector plasmids alone, wt *vpr* plasmid plus *HSP42*-expressing plasmid, wt *vpr* plasmid plus *HSP26*-expressing plasmid, and wt *vpr* plasmid plus library vector plasmid. Two independent transformants are shown for each combination.

HSP42 and *HSP42* regions, respectively, were deleted, failed to suppress. In order to test specifically whether the *HSP42* ORF was required for suppression, one additional mutant was constructed. The plasmid pJG1498 was restricted at the unique *Nde*I site, and the 5′ overhang was filled in, resulting in a 2-bp insertion and a +1 frameshift in the *HSP42* ORF at codon 155 (pJG1501). The modified sequence was predicted to encode a protein of 199 amino acids. This *HSP42* frameshift mutant (pJG1501) did not suppress Vpr toxicity (Fig. 3A). Cells expressing both Vpr and Hsp42p were examined by phalloidin-TRITC staining and fluorescence microscopy in order to determine whether the cytoskeletal disruption observed in cells expressing Vpr alone was reversed by Hsp42p expression. As shown in Fig. 2D, cells expressing Hsp42p and Vpr had a normal cytoskeleton staining pattern. Thus, *HSP42* expression suppressed the growth and cytoskeletal defects associated with Vpr expression.

HSP42 encodes a 376-amino-acid member of the class of sHSPs. The region upstream of *HSP42* contains *cis*-acting heat shock and stress elements which bind *trans*-acting regulators of stress response genes (17). Because Hsp42p has some similarity to Hsp26p in the α-crystallin motif, it was of interest to determine whether suppression of the effects of Vpr expression was also mediated by Hsp26p.

HSP26 was amplified from genomic DNA by PCR and cloned into the high-copy-number, *LEU2*-marked library vector, YEp351, used to identify *HSP42*, resulting in pJG1504. Cells transformed with the plasmid from which wt Vpr was expressed under *GAL1* promoter control and with the plasmid carrying *HSP26* were streaked onto SG medium lacking leucine and uracil to select for the two plasmids and to induce Vpr expression. As shown in Fig. 3C, the presence of a high-copy-number plasmid carrying *HSP26* was sufficient to suppress the negative effects of Vpr expression, although the colonies were slightly smaller than those expressing *vpr* and *HSP42.*

Hsp42p does not suppress Vpr effects by decreasing the level of Vpr mRNA or protein. HSPs are involved in the recovery and turnover of aberrant proteins within the cell. Thus, it was possible that Hsp42p suppressed the effect of Vpr by decreasing the level of Vpr in the cell. In order to determine whether this was the case, Northern and immunoblot analyses were performed to monitor the levels of Vpr RNA and protein, respectively, in cells expressing Hsp42p. Cultures of YPH500 transformed with the *vpr* plasmid and the *vpr* mutant plasmid were grown to log phase in raffinose-containing medium lacking uracil and leucine. The cultures were split, and glucose or galactose was added to each half to repress or induce expression of *vpr*, respectively. Growth was resumed for 5 h. Northern blot analysis with a probe specific for *vpr* showed that, as anticipated, *vpr* RNA was present in cells grown on galactose-containing medium but not in cells grown on glucose-containing medium (Fig. 4A). Immunoblot analysis was performed with the IgG fraction of polyclonal rabbit anti-Vpr antiserum. A protein migrating in the approximate position of a 14-kDa protein, as expected for Vpr, was detected in cultures grown in galactose-containing medium but not in the cultures grown in glucose-containing medium (Fig. 4B). The extract from each of the Vpr-expressing cell types showed Vpr protein at approximately the same level. Thus, the presence of a high-copy-number plasmid encoding Hsp42p for a prolonged period was not associated with a significant decrease in the level of Vpr protein.

Actin and Hsp42p localization in cells undergoing moderate heat shock. The phenotype of yeast cells expressing Vpr in the presence or absence of Hsp42p suggested that Hsp42p stabilized the yeast cytoskeleton. As noted above, sHSPs colocalize with actin in muscle tissue and are associated with increased stability of stress fibers in tissue culture cells (14). In addition, human Hsp27 is concentrated together with actin in the cellular periphery, although the staining pattern does not appear to be the same as that of actin (32). It was therefore of interest to

determine whether Hsp42p colocalized with components of the cytoskeleton under stress conditions.

Indirect immunofluorescence (42) was used to determine the cellular localization of Hsp42p. Rabbit polyclonal anti-Hsp42p IgG reacted with a secondary FITC-conjugated goat anti-rabbit IgG was used to visualize Hsp42p. The polyclonal anti-Hsp42p IgG fraction reacted with two proteins of an apparent mass of about 42 kDa in immunoblots of YPH500 WCE, but not in WCE of the isogenic Δ*hsp42* strain. YPH500 cells were grown to log phase at 23°C in YPD medium in a shaking water bath. Cells maintained at 23°C or heat shocked by shifting to 39°C in a shaking water bath were collected at 0, 10, 30, 60, and 90 min in order to examine localization of Hsp42p in normal and heat-shocked cells. DNA was stained by the addition of DAPI to visualize nuclei. In cells maintained at 23°C, no Hsp42p reactivity was observed (data not shown). At times from 30 to 90 min after the heat shock, intensely staining spots which did not coincide with the nuclei or mitochondria visualized by DAPI staining were observed (data not shown; see below).

The relative localization of Hsp42p and actin was determined by immunofluorescence. Cells were grown at 23°C to log phase and were shifted to 39°C as described above. Samples were collected from cultures maintained at 23°C and from cultures shifted to 39°C for 60 min. Cells were fixed and stained with rabbit anti-Hsp42p antibody and FITC-conjugated goat anti-rabbit IgG and with mouse monoclonal anti-actin antisera and TRITC-conjugated goat anti-mouse IgG. In cells grown at 23°C, actin structure was normal, with the actin patches concentrated in buds and the actin cables in mother cells (data not shown). In cells shifted to 39°C, the normal actin cytoskeletal structure was disrupted. Cortical actin patches were deposited randomly in both mother and daughter cells, and no actin cables were observed in either mother or daughter cells. Although some actin spots colocalized with Hsp42p staining, the signals were distinct overall (Fig. 5). No Hsp42p staining was observed in Δ*hsp42* cells or in cells not subjected to heat shock (data not shown). Control exposures in which a single fluorochrome was photographed with the filter cube for the other fluorochrome, with an exposure time twice as long as that used in the double immunofluorescence experiments, showed no signal, indicating that background fluorescence was not responsible for the appearance of colocalization.

Restoration of actin cables in cells subjected to mild heat shock is more rapid in wt than in Δ*hsp42* cells. Yeast cells shifted from 23 to 39°C arrest growth but eventually resume growth at the elevated temperature. F actin staining was monitored in wt and Δ*hsp42* cells maintained at 39°C to determine whether expression of Hsp42p affected the integrity of the cytoskeleton in cells undergoing stress. A yeast culture in log phase was shifted from 23 to 39°C. At time zero and 10 min, 1 h, 2 h, 3 h, and 4 h after the shift, aliquots of cells were taken and cells were fixed and stained in suspension with TRITC-phalloidin. At 23°C, F actin cables in mother cells were oriented toward the nascent bud. Cortical patches of actin in cells with small buds localized almost exclusively to the bud in both wt and Δ*hsp42* cells (Fig. 6A and E). Within 10 min after the shift, actin cables in mother cells were partially disrupted (Fig. 6B and F). By 1 h after the shift, cortical actin patches had delocalized from the daughter cell to the mother cell and actin filament cables had disappeared from the mother cells in both wt and Δ*hsp42* populations (Fig. 6C and G). At 3 h, in 88% of wt cells with small buds, the cellular location of TRITC-phalloidin-stained actin was similar to that observed in non-heat-shocked cells (Fig. 6D), while only 34% of the Δ*hsp42* cells showed restored actin structure (Fig. 6H). Differences were

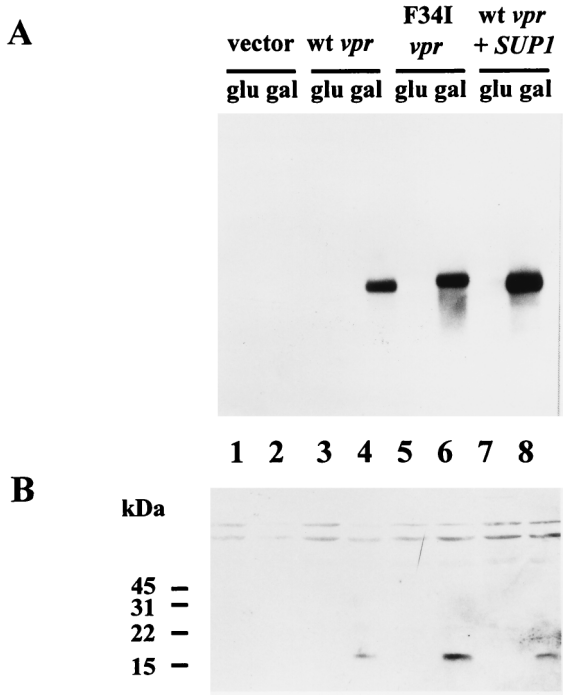

FIG. 4. Immunoblot and Northern blot analyses of cells expressing wt *vpr*, F34I *vpr*, and wt *vpr* plus suppressor. RNA (A) or protein (B) was extracted from cultures containing vector plasmids (lanes 1 and 2), wt *vpr* and vector plasmids (lanes 3 and 4), F34I *vpr* and vector plasmids (lanes 5 and 6), and wt *vpr* and *SUP1* plasmids (lanes 7 and 8). Extracts shown in lanes 1, 3, 5, and 7 were from cells grown in glucose-containing medium which repressed *vpr* expression. Extractions shown in lanes 2, 4, 6, and 8 were from cells grown in galactose-containing medium which induced *vpr* expression. Total RNA was isolated and fractionated by electrophoresis on a 1.1% agarose gel, blotted onto a nylon filter, and detected with a *vpr*-specific probe. Ten micrograms of total protein was fractionated by electrophoresis on 15% polyacrylamide-SDS gels, electroblotted, and probed with the IgG fraction of anti-Vpr antisera.

quantitated by determining the proportion of cells with small buds which contained actin cables for each time point in two different experiments (Fig. 6I). The percentage of recovered Δ*hsp42* cells after 4 h was about half the percentage of recovered wt cells. The level of Hsp42p protein in cells at 0 to 3 h was determined by immunoblot analysis with anti-Hsp42p antibodies in order to determine how closely the induction of Hsp42p protein corresponded to the cytoskeletal recovery from the temperature shift. Wt and Δ*hsp42* cells were shifted from 23 to 39°C. Samples were collected at 0, 1, 2, and 3 h after the temperature shift, and protein was extracted. Immunoblot analysis of equal amounts of WCE protein from cells at these time points with the IgG fraction of anti-Hsp42p antisera showed two proteins of approximately 42 kDa which were unique to cells expressing Hsp42p. Bands representing each of these species appeared to increase in intensity with the shift to elevated temperature. Examination of these species over the time course showed that the amount of Hsp42p increased dramatically by 1 h after the shock and remained elevated 3 h after the shock (Fig. 7).

DISCUSSION

Expression of HIV-1 Vpr in budding yeast causes the accumulation of cells with cytoskeletal defects and a slow-growth phenotype. A gene encoding an sHSP was isolated as a suppressor of the slow-growth phenotype. The function of the

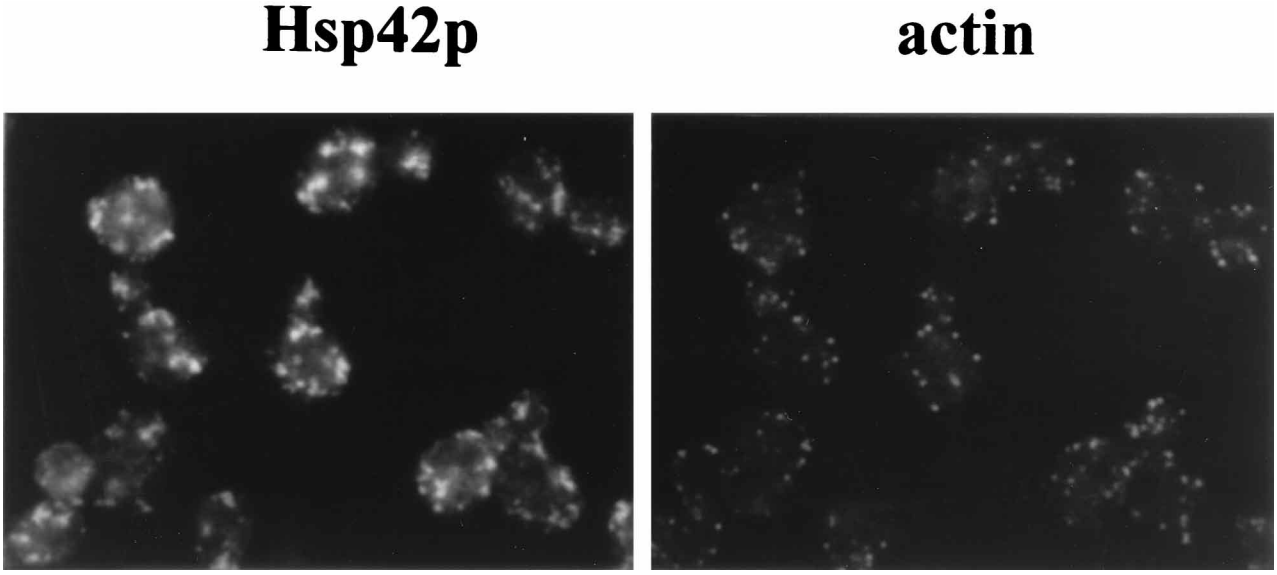

FIG. 5. Subcellular localization of Hsp42p and actin in cells undergoing heat shock. YPH500 cells were grown to log phase at 23°C and were shifted to 39°C. Samples were collected from cultures 60 min after the shift to 39°C. Cells were prepared as described in Materials and Methods and were stained with rabbit anti-Hsp42p antibody and FITC-conjugated goat anti-rabbit IgG (for visualization of Hsp42p) and with mouse antiactin antibody and TRITC-conjugated goat anti-mouse IgG (for visualization of actin).

sHSP was investigated for two reasons. First, we were intrigued that a member of this class of proteins, previously implicated in stress fiber stabilization, could reverse the phenotype caused by *vpr* expression. If the effect of Vpr could be reversed by a protein which stabilizes the cytoskeleton, this would imply, although not prove, a primary effect of Vpr on the cytoskeleton rather than on some global regulator of cell growth. The most marked phenotype previously reported for sHSP expression in yeast was reduced survival of Δ*hsp42* cells after 5 months at 4°C (from 10.8% for wt cells to 6.7% for Δ*hsp42*) (56) and very modest increased survival at elevated temperatures of cells overexpressing *HSP26* (8, 51). The suppression of Vpr offered a phenotype, albeit an artificial one, which was more amenable to investigation of the function of Hsp42p.

Expression of Vpr and the concomitant G_2 arrest in animal cells correlate with accumulation of a phosphorylated, inactive form of $p34^{cdc2}$. In addition to the observation by Macreadie et al. (36) that Vpr expression in budding yeast caused morphological abnormalities, it has recently been reported that Vpr expression in fission yeast causes morphological abnormalities and accumulation of phosphorylated, inactive $p34^{cdc2}$ (57). In human cells and in fission yeast, okadaic acid, an inhibitor of PP2A and PP1 phosphatases, which act indirectly to inactivate Cdc2p, reverses or attenuates the effect of Vpr expression (44, 57), and in human cells, introduction of a mutant Cdc2p that cannot be phosphorylated also reverses the effects of Vpr (24). Thus, one interpretation of the observations made in mammalian and *Schizosaccharomyces pombe* systems has been that Vpr acts upstream of Cdc2p activation by preventing its dephosphorylation. However, some findings have suggested that regulation of Cdc28p (the Cdc2p homolog) in *S. cerevisiae* is not analogous to that observed in mammalian cells and in *S. pombe*. For example, mutations in *CDC28* changing the tyrosine which is phosphorylated in mammalian p34 or *S. pombe* Cdc2p do not result in a small-cell phenotype in *S. cerevisiae* (3, 49). This result implies that this residue is not normally used to negatively regulate Cdc28p. Thus, although the phenotype we observed could be caused by perturbation of regulation upstream of Cdc28p, it is not the same as the G_2 arrest observed in fission yeast and animal cells.

In the experiments described in this report, Vpr was expressed at high levels in cells of a nonhost species. Thus, it could have novel effects in place of, or in addition to, its native activities. If regulation of phosphorylation were disrupted by direct interaction between Vpr and global regulators in budding yeast and if Hsp42p were operating to directly stabilize the cytoskeleton, it is initially surprising to consider that the Vpr effect could be reversed by expression of sHSP. Although sHSPs are linked to stress and mitogen signalling pathways, they are thought to function as targets of kinase cascades (4). Nevertheless, Hsp42p suppression of Vpr effects does not exclude a role for Vpr in affecting global phosphorylation in *S. cerevisiae*. There is evidence that mammalian sHSPs are phosphorylated by mitogen-activated protein kinase-activated protein (MAPKAP) kinase 2 (47, 50) and dephosphorylated by PP2A (11). Thus, Hsp42p could act as a sink for phosphorylation or phosphatase activity and have indirect effects on the state of phosphorylation of other proteins. Alternatively, if Vpr disrupts the function of structural proteins which are monitored by checkpoint control, those structural proteins could be targets of Hsp42p function. MacCreadie et al. (36) noted a similarity between Vpr and a region of Sac1p, the gene for which was isolated as a suppressor of an actin defect in yeast (13). If Vpr disrupts the cytoskeleton by interfering with Sac1p, then Hsp42p might bypass the effect by stabilizing actin polymers.

Although effects of ectopic expression of sHSP have been documented in animal cell culture, only modest differences in viability between cultures of wt and *hsp12 hsp26* or *hsp26 hsp42* mutant cells have been observed in yeast. Nor has overexpression of Hsp12p or Hsp26p resulted in more than marginal effects on cells undergoing stress. Thus, although it was a synthetic phenotype, the rescue of cells expressing Vpr by a high-copy-number plasmid carrying the gene for an sHSP was the first instance in which expression of an sHSP had been shown to confer a phenotype in yeast affecting more than a

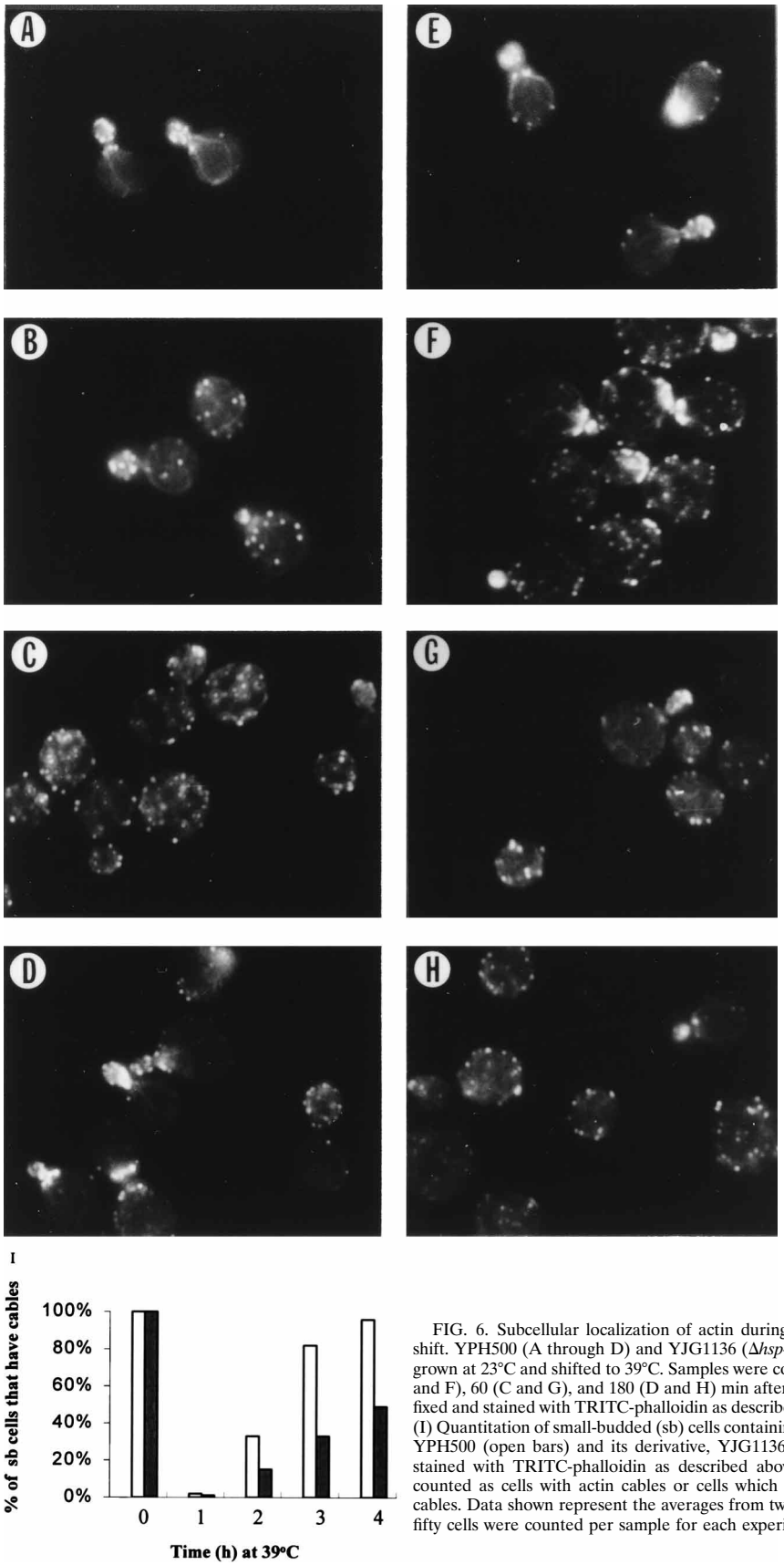

FIG. 6. Subcellular localization of actin during recovery from temperature shift. YPH500 (A through D) and YJG1136 (Δ*hsp42*) (E through H) cells were grown at 23°C and shifted to 39°C. Samples were collected at 0 (A and E), 10 (B and F), 60 (C and G), and 180 (D and H) min after the shift to 39°C. Cells were fixed and stained with TRITC-phalloidin as described in Materials and Methods. (I) Quantitation of small-budded (sb) cells containing actin cables. Cells of strain YPH500 (open bars) and its derivative, YJG1136 (Δ*hsp42*) (solid bars), were stained with TRITC-phalloidin as described above. Small-budded cells were counted as cells with actin cables or cells which did not have apparent actin cables. Data shown represent the averages from two experiments. One hundred fifty cells were counted per sample for each experiment.

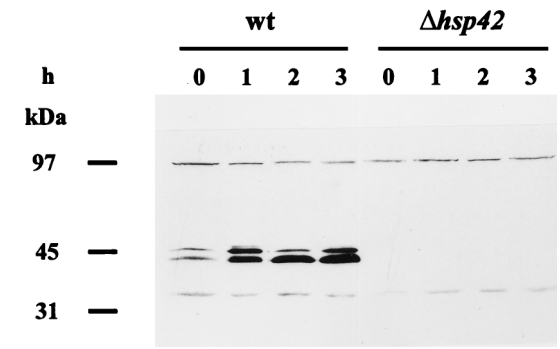

FIG. 7. Analysis of Hsp42p synthesis in cells undergoing heat shock. YPH500 or YJG1136 (Δ*hsp42*) cells were grown to log phase at 23°C and shifted to 39°C. Samples were collected at 0, 1, 2, and 3 h after the shift. Whole-cell proteins were extracted from samples. Ten micrograms of total protein was fractionated by electrophoresis on SDS–10% polyacrylamide gels, electroblotted, and probed with anti-Hsp42p IgG.

small percentage of the population. In cells undergoing stress, although Hsp42p did not generally colocalize with actin, there were some regions of overlapping staining. Hsp42p could not be visualized in cells overexpressing *HSP42* under galactose regulation. Because the actin cytoskeleton was disrupted in cells where Hsp42p could be visualized, it is difficult to assess the implications of these data for Hsp42p and actin interaction. Although sHSPs have not been previously implicated in actin function in vivo in yeast cells, our study suggests that Hsp42p promotes restoration of the cytoskeleton during mild stress.

A role for sHSPs in poststress actin reorganization has not been directly examined in animal cells. Although the staining pattern for sHSPs is somewhat diffuse in animal cells in culture, it appears to concentrate in regions of cytoskeletal activity (32). In cardiac muscle sHSPs colocalize with actin (34). In culture cells, increased stress resistance conferred by ectopic sHSP expression correlates with increased stability of stress fibers (31). Avian and yeast sHSPs have been shown to inhibit actin polymerization in vitro (39, 40, 43), and studies with a murine sHSP showed that this ability to interfere with actin polymerization is regulated by phosphorylation and multimerization (7). Thus, sHSPs could participate in regulated effects on the cytoskeleton in response to stress and mitogens. Synthesis of actin and tubulin structures is particularly sensitive to defects in the chaperonin complex (12, 33). In addition, yeast actin mutants are sensitive to high osmolarity (55). The induction of sHSPs in cells undergoing osmotic shock could serve to stabilize actin if the cytoskeleton is sensitive to changes in osmolarity. The sHSPs have also been shown to have chaperone activity in vitro, although this has not been demonstrated in vivo. We hypothesize that sHSPs act as chaperones for mature actin during its disassembly-reassembly in cells undergoing stress.

This screen for suppressors of the effect of Vpr expression in yeast resulted in the identification of members of two classes of proteins, some of which are likely to act on the cytoskeleton (this study and unpublished data). The facts that Vpr disrupts the yeast cytoskeleton and that this effect can be reversed by an sHSP suggest unanticipated ways in which Vpr could interact with host cells. The serendipitous discovery of Vpr and physiological phenotypes related to a yeast sHSP will facilitate genetic screens for the molecules which modulate and respond to this interesting class of proteins.

ACKNOWLEDGMENTS

This work was supported by a grant from the Universitywide AIDS Task Force of the University of California to S.B.S. and R01 AI30927 to M.E.

We thank J. Loeb and S. Demaggio for assistance in the fluorescence-activated cell sorting analysis and H. Liu and J. Loeb for helpful discussions. We particularly thank R. Sandri-Goldin for the use of her Nikon microscope.

REFERENCES

1. **Alani, E., L. Cao, and N. Kleckner.** 1987. A method for gene disruption that allows repeated use of *URA3* selection in the construction of multiply disrupted yeast strains. Genetics **116:**541–545.
2. **Altschul, S. F., W. Gish, W. Miller, E. W. Myers, and D. J. Lipman.** 1990. Basic local alignment search tool. J. Mol. Biol. **215:**403–410.
3. **Amon, A., U. Surana, I. Muroff, and K. Nasmyth.** 1992. Regulation of $p34^{CDC28}$ tyrosine phosphorylation is not required for entry into mitosis in *S. cerevisiae*. Nature **355:**365–368.
4. **Arrigo, A., and J. Landry.** 1994. Expression and function of the low-molecular-weight heat shock proteins, p. 335–373. *In* R. I. Morimoto, A. Tissieres, and C. Georgopoulos (ed.), The biology of heat shock proteins and molecular chaperones. Cold Spring Harbor Laboratory Press, Cold Spring Harbor, N.Y.
5. **Ausubel, F. M., R. Brent, R. E. Kingston, D. D. Moore, J. G. Seidman, J. A. Smith, and K. Struhl.** 1997. Current protocols in molecular biology. Greene Publishing Associates and Wiley Interscience, New York, N.Y.
6. **Bartz, S. I., M. E. Rogel, and M. E. Emerman.** 1996. HIV-1 Vpr cell cycle control: Vpr is cytostatic and mediates G_2 accumulation by a mechanism which differs from DNA damage checkpoint control. J. Virol. **70:**2324–2331.
7. **Benndorf, R., K. Hayess, S. Ryazantsev, M. Wieske, J. Behlke, and G. Lutsch.** 1994. Phosphorylation and supramolecular organization of murine small heat shock protein HSP25 abolish its actin polymerization-inhibiting activity. J. Biol. Chem. **269:**20780–20784.
8. **Bentley, N. J., I. T. Fitch, and M. F. Tuite.** 1992. The small heat-shock protein Hsp26 of *Saccharomyces cerevisiae* assembles into a high molecular weight aggregate. Yeast **8:**95–106.
9. **Bouhamdan, M., S. Benichou, F. Rey, J.-M. Navarro, I. Agostini, B. Spire, J. Camonis, G. Slupphaug, R. Vigne, R. Benarous, and J. Sire.** 1996. Human immunodeficiency virus type 1 Vpr protein binds to the uracil DNA glycosylase DNA repair enzyme. J. Virol. **70:**697–704.
10. **Bradford, M. M.** 1976. A rapid and sensitive method for the quantitation of microgram quantities of protein utilizing the principle of protein-dye binding. Anal. Biochem. **72:**248–254.
11. **Cairns, J., S. Qin, R. Philp, Y. H. Tan, and G. R. Guy.** 1994. Dephosphorylation of the small heat shock protein Hsp27 in vivo by protein phosphatase 2A. J. Biol. Chem. **269:**9176–9183.
12. **Chen, X., D. S. Sullivan, and T. C. Huffaker.** 1994. Two yeast genes with similarity to TCP-1 are required for microtubule and actin function *in vivo*. Proc. Natl. Acad. Sci. USA **91:**9111–9115.
13. **Cid, V. J., A. Duran, F. del Rey, M. P. Snyder, C. Nombela, and M. Sanchez.** 1995. Molecular basis of cell integrity and morphogenesis in *Saccharomyces cerevisiae*. Microbiol. Rev. **59:**345–386.
14. **Ciocca, D. R., S. Oesterreich, G. C. Chamness, W. L. McGuire, and S. A. W. Fuqua.** 1993. Biological and clinical implications of heat shock protein 27000 (Hsp27): a review. J. Natl. Cancer Inst. **85:**1558–1570.
15. **Clark, D. J., V. W. Bilanchone, L. J. Haywood, S. L. Dildine, and S. B. Sandmeyer.** 1988. A yeast sigma composite element, Ty3, has properties of a retrotransposon. J. Biol. Chem. **263:**1413–1423.
16. **Colicelli, J., C. Nicolette, C. Birchmeir, L. Rodgers, M. Riggs, and M. Wigler.** 1991. Expression of three mammalian cDNAs that interfere with RAS function in *Saccharomyces cerevisiae*. Proc. Natl. Acad. Sci. USA **88:**2913–2917.
17. **Craig, E. A., B. D. Gambill, and R. J. Nelson.** 1993. Heat shock proteins: molecular chaperones of protein biogenesis. Microbiol. Rev. **57:**402–414.
18. **Emerman, M.** 1996. HIV-1 Vpr and the cell cycle. Curr. Biol. **6:**1096–1103.
19. **Engebrecht, J., J. Hirsch, and G. S. Roeder.** 1990. Meiotic gene conversion and crossing over: their relationship to each other and to chromosome synapsis and segregation. Cell **62:**927–937.
20. **Feinberg, A. P., and B. Vogelstein.** 1983. A technique for radiolabeling DNA restriction endonuclease fragments to high specific activity. Anal. Biochem. **132:**6–13. (Addendum, **137:**266–267, 1984.)
21. **Fletcher, T. M., B. Brichachek, N. Sharova, S. McPherson, G. Stivahtis, P. Sharp, M. Emerman, B. Hahn, and M. Stevenson.** 1996. Nuclear import and cell cycle arrest functions of the HIV-1 Vpr protein are encoded by two separate genes in HIV-2/SIV_{SM}. EMBO J. **15:**6155–6165.
22. **Gallay, P., V. Stitt, C. Mundy, M. Oettinger, and D. Trono.** 1996. Role of the karyopherin pathway in human immunodeficiency virus type 1 nuclear import. J. Virol. **70:**1027–1032.
23. **Guthrie, C., and G. R. Fink (ed.).** 1991. Methods in enzymology, vol. 194. Guide to yeast genetics and molecular biology. Academic Press, Inc., San Diego, Calif.

24. **He, J., S. Choe, R. Walker, P. DiMarzio, D. O. Morgan, and N. R. Landau.** 1995. Human immunodeficiency virus type 1 viral protein R (Vpr) arrests cells in the G_2 phase of the cell cycle by inhibiting $p34^{cdc2}$ activity. J. Virol. **69:**6705–6711.
25. **Heinzinger, N. K., M. I. Bukinsky, S. A. Haggerty, A. M. Ragland, V. Kewalramani, M. A. Lee, H. E. Gendelman, L. Ratner, M. Stevenson, and M. Emerman.** 1994. The Vpr protein of human immunodeficiency virus type 1 influences nuclear localization of viral nucleic acids in nondividing host cells. Proc. Natl. Acad. Sci. USA **91:**7311–7315.
26. **Ito, H., Y. Fukuda, K. Murata, and A. Kimura.** 1983. Transformation of intact yeast cells treated with alkali cations. J. Bacteriol. **153:**163–168.
27. **Jakob, U., M. Gaestel, K. Engel, and J. Buchner.** 1993. Small heat shock proteins are molecular chaperones. J. Biol. Chem. **268:**1517–1520.
28. **Jowett, J. B. M., V. Planelles, B. Poon, N. P. Shah, M.-L. Chen, and I. S. Y. Chen.** 1995. The human immunodeficiency virus type 1 *vpr* gene arrests infected T cells in the G_2 + M phase of the cell cycle. J. Virol. **69:**6304–6313.
29. **Kewalramani, V. N., C. Park, P. Gallombardo, and M. Emerman.** 1996. Protein stability influences human immunodeficiency virus type 2 Vpr virion incorporation and cell cycle effect. Virology **218:**326–334.
30. **Kurtz, S., J. Rossi, L. Petko, and S. Lindquist.** 1986. An ancient developmental induction: heat-shock proteins induced in sporulation and oogenesis. Science **231:**1154–1157.
31. **Lavoie, J. N., G. Gingras-Breton, R. M. Tanguay, and J. Landry.** 1993. Induction of Chinese hamster HSP27 gene expression in mouse cells confers resistance to heat shock. J. Biol. Chem. **268:**3420–3429.
32. **Lavoie, J. N., E. Hickey, L. A. Weber, and J. Landry.** 1993. Modulation of actin microfilament dynamics and fluid phase pinocytosis by phosphorylation of heat shock protein 27. J. Biol. Chem. **268:**24210–24214.
33. **Lewis, S. A., G. Tian, I. E. Vainberg, and N. J. Cowan.** 1996. Chaperonin-mediated folding of actin and tubulin. J. Cell Biol. **132:**1–4.
34. **Longoni, S., S. Lattonen, G. Bullock, and M. Chiesi.** 1990. Cardiac alpha-crystallin: intracellular localization. Mol. Cell. Biochem. **97:**121–128.
35. **Macreadie, I. G., C. K. Arunagiri, D. R. Hewish, J. F. White, and A. A. Azad.** 1996. Extracellular addition of a domain of HIV-1 Vpr containing the amino acid sequence motif H(S/F)RIG causes cell membrane permeabilization and death. Mol. Microbiol. **19:**1185–1192.
36. **Macreadie, I. G., L. A. Castelli, D. R. Hewish, A. Kirkpatrick, A. C. Ward, and A. A. Azad.** 1995. A domain of human immunodeficiency virus type 1 Vpr containing repeated H(S/F)RIG amino acid motifs causes cell growth arrest and structural defects. Proc. Natl. Acad. Sci. USA **92:**2770–2774.
37. **McMaster, G. K., and G. G. Carmichael.** 1977. Analysis of single- and double-stranded nucleic acids on polyacrylamide and agarose gels by using glyoxal and acridine orange. Proc. Natl. Acad. Sci. USA **74:**4835–4838.
38. **Menees, T. M., and S. B. Sandmeyer.** 1994. Transposition of the yeast retroviruslike element Ty3 is dependent on the cell cycle. Mol. Cell Biol. **14:**8229–8240.
39. **Miron, T., K. Vancompernolle, J. Vandekerckhove, M. Wilchek, and B. Geiger.** 1991. A 25 kD inhibitor of actin polymerization is a low molecular mass heat shock protein. J. Cell Biol. **114:**255–261.
40. **Miron, T., M. Wilchek, and B. Geiger.** 1988. Characterization of an inhibitor of actin polymerization in vinculin-rich fraction of turkey gizzard smooth muscle. Eur. J. Biochem. **178:**543–553.
41. **Praekelt, U. M., and P. A. Meacock.** 1990. *HSP12*, a new small heat shock gene of *Saccharomyces cerevisiae*: analysis of structure, regulation and function. Mol. Gen. Genet. **223:**97–106.
42. **Pringle, J. R., R. A. Preston, A. E. M. Adams, T. Stearns, D. G. Drubin, B. K. Haarer, and E. W. Jones.** 1989. Fluorescence microscopy methods for yeast. Methods Cell Biol. **31:**357–435.
43. **Rahman, R. R. J., N. J. Bentley, and M. F. Tuite.** 1995. The *Saccharomyces cerevisiae* small heat shock protein Hsp26 inhibits actin polymerisation. Biochem. Soc. Trans. **77S:**23.
44. **Re, F., D. Braaten, E. K. Franke, and J. Luban.** 1995. Human immunodeficiency virus type 1 Vpr arrests the cell cycle in G_2 by inhibiting the activation of $p34^{cdc2}$-cyclin B. J. Virol. **69:**6859–6864.
45. **Refaeli, Y., D. N. Levy, and D. B. Weiner.** 1995. The glucocorticoid receptor type II complex is a target of the HIV-1 *vpr* gene product. Proc. Natl. Acad. Sci. USA **92:**3621–3625.
46. **Rogel, M. E., L. I. Wu, and M. Emerman.** 1995. The human immunodeficiency virus type 1 *vpr* gene prevents cell proliferation during chronic infection. J. Virol. **69:**882–888.
47. **Rouse, J., P. Cohen, S. Trignon, M. Morange, A. Alonso-Llamazares, D. Zamanillo, T. Hunt, and A. R. Nebreda.** 1994. A novel kinase cascade triggered by stress and heat shock that stimulates MAPKAP kinase-2 and phosphorylation of the small heat shock proteins. Cell **78:**1027–1037.

47a. **Selig, L., S. Benichou, M. E. Rogel, L. I. Wu, M. A. Vodicka, J. Sire, R. Benarous, and M. Emerman.** 1997. Uracil DNA glycosylase specifically interacts with Vpr of both human immunodeficiency virus type 1 and siman immunodeficiency virus of sooty mangabeys, but binding does not correlate with cell cycle arrest. J. Virol. **71:**4842–4846.

48. **Sikorski, R., and P. Hieter.** 1989. A uniform set of multipurpose shuttle vectors and yeast host strains designed for efficient manipulation of DNA in *Saccharomyces cerevisiae*. Genetics **122:**19–27.
49. **Sorger, P. K., and A. W. Murray.** 1992. S-phase feedback control in budding yeast independent of tyrosine phosphorylation of p34*CDC28*. Nature **355:**365–368.
50. **Stokoe, D., K. Engel, D. G. Campbell, P. Cohen, and M. Gaestel.** 1992. Identification of MAPKAP kinase 2 as a major enzyme responsible for the phosphorylation of the small mammalian heat shock proteins. FEBS Lett. **313:**307–313.
51. **Susek, R. E., and S. L. Lindquist.** 1989. hsp26 of *Saccharomyces cerevisiae* is related to the superfamily of small heat shock proteins but is without a demonstrable function. Mol. Cell. Biol. **9:**5265–5271.
52. **Thomas, P. S.** 1980. Hybridization of denatured RNA and small DNA fragments transferred to nitrocellulose. Proc. Natl. Acad. Sci. USA **77:**5201–5205.
53. **Towbin, H., and J. Gordon.** 1984. Immunoblotting and dot-blotting—current status and outlook. J. Immunol. Methods **72:**313–340.
54. **Wang, L., S. Mukherjee, F. Jia, O. Narayan, and L. Zhao.** 1995. Interaction of virion protein Vpr of human immunodeficiency virus type 1 with cellular transcription factor Sp1 and trans-activation of viral long terminal repeat. J. Biol. Chem. **270:**25564–25569.
55. **Wertman, K. F., D. G. Drubin, and D. Botstein.** 1992. Systematic mutational analysis of the yeast *ACT1* gene. Genetics **132:**337–350.
56. **Wotton, D., K. Freeman, and D. Shore.** 1996. Multimerization of Hsp42p, a novel heat shock protein of *Saccharomyces cerevisiae*, is dependent on a conserved carboxyl-terminal sequence. J. Biol. Chem. **271:**2717–2723.
57. **Zhao, Y., J. Cao, M. R. G. O'Gorman, M. Yu, and R. Yogev.** 1996. Effect of human immunodeficiency virus type 1 protein R (*vpr*) gene expression on basic cellular function of fission yeast *Schizosaccharomyces pombe*. J. Virol. **70:**5821–5826.